Polymeric Waveguide Based Integrated Optical Signal Processing Circuits

Xuejun Lu [1] and Ray T. Chen [2]
[1] University of Massachusetts Lowell, [2] University of Texas at Austin

ABSTRACT

All-Optical signal processing and routing avoid the optical-to-electrical and electrical-to-optical conversions and thus eliminates the bandwidth constrains set by conventional electronics technologies. It will form key building blocks for the next generation ultra-high speed and dynamic multi-casting optical networks. Polymer waveguide based photonics integrated circuits are promising in achieving high-performance optical signal processing circuits due to their large Electro-optic/thermo-optic coefficients and structure flexibility. In this paper, design examples such as dynamic channel equalizer, optical CDMA encoder and matched filter are analyzed. Simulation results are presented.

Keywords: DWDM, Adaptive Filter, All-optical processing, Thermo-optics, Electro-optics, Polymer Waveguide, Variable Attenuator, Optical filter,

1. INTRODUCTION

The state-of-the-art electronic signal processing speeds have fallen far behind the capabilities of both optical time-division multiplexing (TDM) and wavelength-division multiplexing (WDM) systems [1]. Ultra-high speed electric circuits (>40GHz) become impossible to achieve with conventional integrated circuits, even when pushed to the state-of-the-art in lithography [2]. The processing speed limit of state-of-the-art electronic circuits seriously constrains the data transport bandwidth for telecommunication or data communications involving electronics processing or controlling, such as signal reshaping and routing in a multi-casting network. Performing signal-processing operations entirely within the optical domain, i.e. all-optical signal processing, would exploit the speed and parallelism inherent to optics. This all-optical processing technology avoids the electrical-to-optical and optical-to-electrical conversions and thus eliminates the bandwidth constrains set by conventional electronics technologies. It is expected to provide ultra-high communication bandwidth that is beyond the limit of conventional electronics counterparts. In addition, it offers simplified architectures for photonic networks [3] and reduces the overall costs for network maintenance and upgrading. Because of this, the all-optical signal processing technology will play an important role in the next generation fiber-to-the-home (FTTH) [4] photonic packet-switched networks [5].

Despite the potential advantages, the all-optical signal processing technology is still at a relatively immature stage of development. One of the key issues relates to the lack of reliable and cost-effective integrated optical platform. Whereas all-optical signal processing components such as all-optical analog-to-digital converter, hard-limiter, buffer

Active and Passive Optical Components for WDM Communications IV, edited by
Achyut K. Dutta, Abdul Ahad S. Awwal, Niloy K. Dutta, Yasutake Ohishi, Proc. of SPIE
Vol. 5595 (SPIE, Bellingham, WA, 2004) · 0277-786X/04/$15 · doi: 10.1117/12.570804

and ring-resonators have been developed [6-9], integrated all-optical signal processing circuits that can perform desired functions including pulse shaping and signal routing are still unavailable due to the difficulties of obtaining the accurate time-delay lines and tunable phase-shifter as well as achieving reduced interference noises in reliable and cost-effective integrated optical platform.

To overcome these limitations, we proposed integrated all-optical circuits based polymer waveguide technology to employ the large thermo-optic (TO) and electro-optic (EO) coefficients provided by organic EO materials and the flexibility of fabrication and packing of polymer photonic devices. The combination of the large nonlinear optical coefficients, including TO and EO, and the fabrication flexibility provides a unique approach to achieve enhanced optical signal processing functions such as pulse shaping, encoding and optical signal routing. In the paper, all-optical signal processing circuit design examples based on polymeric integrated circuits, including dynamic channel equalizer, optical CDMA encoder and matched filter, are presented. Simulation results are analyzed with further discussions of their application in optical signal processing.

2. DYNAMIC CHANNEL EQUALIZER

Spectral equalization is an essential technology to compensate for erbium-doped fiber amplifier (EDFA) uneven gain and power fluctuations in individual 100-GHz-wavelength spacing dense wavelength-division-multiplexing (DWDM) channels due to dynamically adding, dropping and routing of these channels [10, 11]. We have developed a dynamic gain equalizer based on polymeric photonics integrated circuits with attractive features such as: modular structure, low sensitivity to parameter quantization errors, and simple method to ensure filter stability [10]. The schematic drawing of the dynamically tunable gain equalizer shown in Fig. 2.1,

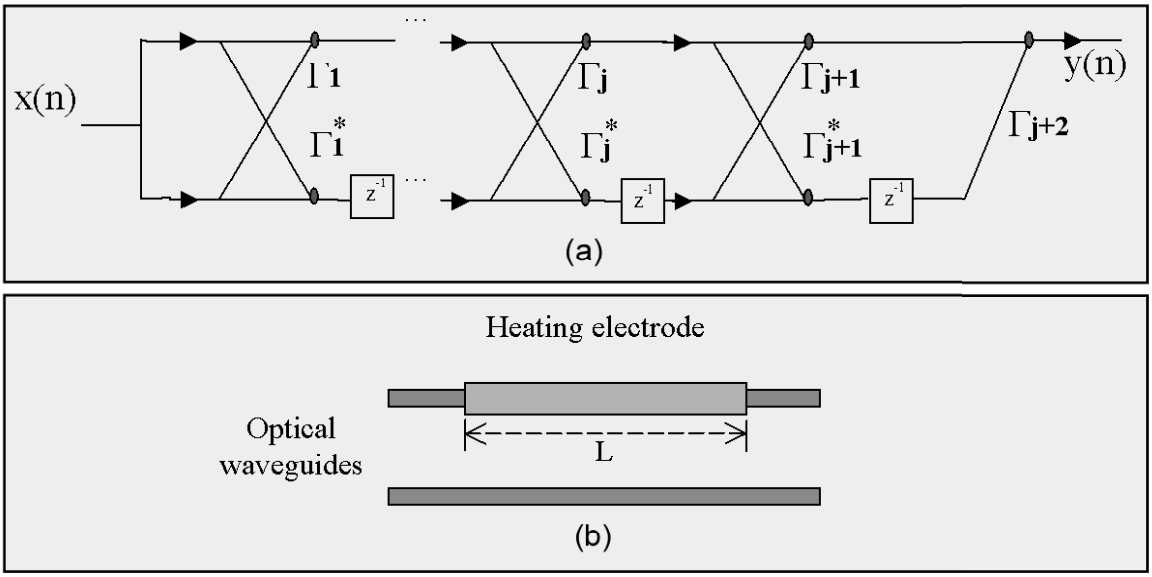

Fig. 2.1, Schematic drawing the dynamically tunable gain equalizer based on polymeric photonics integrated circuit: (a) Lattice filter structure; (b) thermo-optical tunable delay lines.

The dynamically tunable gain equalizer consists of several (p) cascaded two-port modules with reflection coefficients Γ1, Γ2 , …, Γp, which forms the pth-order lattice filter. Each stage consists of two inputs, two outputs and a cross structure with a reflection coefficient of Γ, where Z-1 is the time delay, which is implemented using the thermo-optic effect. The connections are typical single mode waveguides, 3 dB couplers and combiners. Γ1, Γ2, ... Γj are reflection coefficients, which can synthesized using the step-down Levison-durbin recursion [12]. Compared with other optical filter structures based on arrayed waveguide grating (AWG) [13] and resonant rings, these two-port optical waveguide structures have no bending structure thus minimize the propagation loss and bending loss caused by the RIE process. The tunable operation was achieved by the thermo-optical lattice filter structure, which consists of two-parallel-optical-waveguides and a heating electrode on one of the waveguides, shown in Fig. 2.1 (b). When the upper waveguide was heated by the top electrode, the index of the waveguide is decrease due to the negative coefficient of the polymer materials. The speed of light pulse traveling in upper waveguide is higher that in the lower arm. The time delay can be written as: $\Delta T = (L/c)\Delta n$. By engineering the length of the waveguides and Δn, the filter range $\Delta f = 1/\Delta T$ can be as high as 4THz, which covers all 40 100GHz-spacing DWDM channels.

Arbitrary gain equalization profile, e.g. Fig.2.2, can be synthesized using reflection coefficients calculated by the digital filter frequency sampling and step-down Levison-durbin recursion algorithms [12, 10]. A resolution of 0.4nm and dynamic range of 40dB can be achieved by the 12-order lattice filter structure based on the polymer photonics integrated circuits [10]. The least-mean-square (LMS) algorithm [12] can be employed to update the filter coefficients for dynamical gain-equalization.

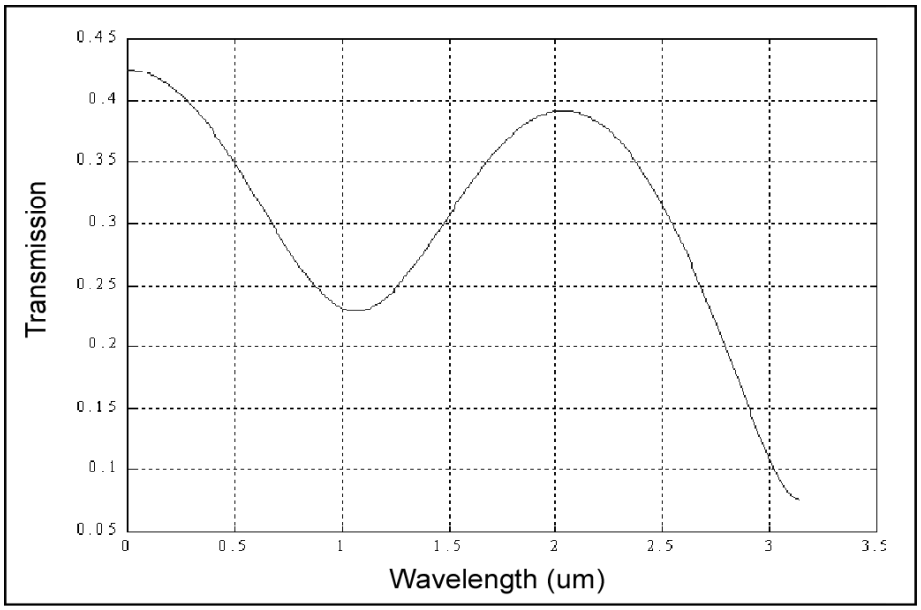

Fig. 2.2. Arbitrary gain equalization profile achieved using the lattice filter structure based on polymer photonics integrated circuits and frequency sampling, step-down Levison-durbin recursion algorithm

3. OPTICAL CDMA ENCODER AND MATCH FILTER

Optical CDMA as an alternative of other optical multiplexing schemes such as wave-length division multiplexing (WDM) and TDM, not only inherits the advantages of microwave CDMA such as efficient bandwidth usage, robust and secure communication over open channels, but also has many additional attractive features including higher granularity and scalability within optical networks, optical transparency to data format and rate, improved cross-talk performance and more flexible asynchronous access [3-8]. In addition, optical CDMA scheme avoids the optical-to-electrical and electrical-to-optical conversion processes and eliminates the bandwidth constrains set by conventional electronics technologies (<10GHz). It offers much higher speed for data transport and routing than electronic counterparts. Due to these advanced features, optical CDMA is a promising technology for next-generation ultra-high speed, cost-effective broadband access network.

One of the potential applications is fiber-to-the-home (FTTH) network. The FTTH based on optical CDMA technology, shown in figure 3.1, provides an ideal solution for the cost and limited available wavelength resource issues associated with TDM and WDM approaches. As shown in figure 3.1, in an optical CDMA based FTTH uplink (form subscriber to central office), voice/video/data are encoded using an OPTICAL CDMA encoder. The encoded data streams from different subscribers are combined through a passive Nx1 combiner and then sent to the central communication office. In an optical CDMA downlink (from central office to individual homes), encoded data streams are split through the 1XN passive splitter and decoded through a predefined access code sequence in each optical CDMA decoder.

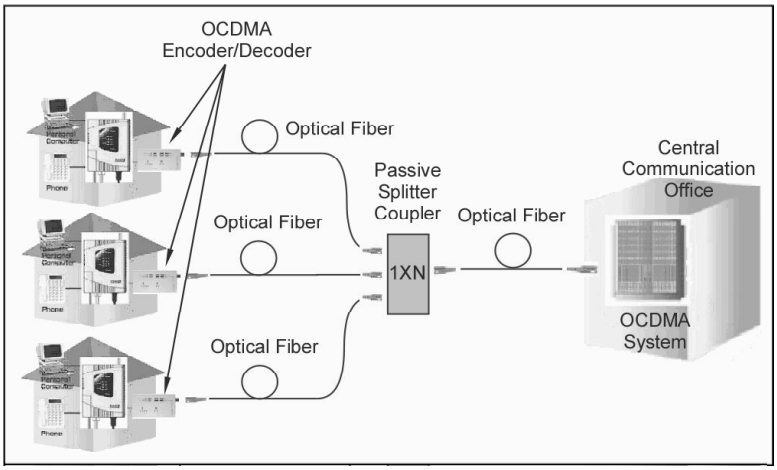

Figure 3.1 Schematic of a fiber-to-the home network based on the OPTICAL CDMA technology

The combination of the large nonlinear optical coefficients, including TO and EO, and the fabrication flexibility offers a unique opportunity for developing integrated optical CDMA encoder and decoder modules that monolithically integrate accurate time-delay lines, tunable phase-shifters, and high-speed time-gates (~20ps). The proposed 10-chip optical CDMA encoder, shown in figure 3.2, consists of eight 10% tap couplers,

optical time-delay lines and eight phase-shifters. Each of the time-delay lines is designed to provide a 10ps time-delay. The time-delayed data streams are phase-encoded by the integrated electro-optic (EO) phase-shifter. The phase-encoded data streams are finally combined and sent out through the optical CDMA output waveguide.

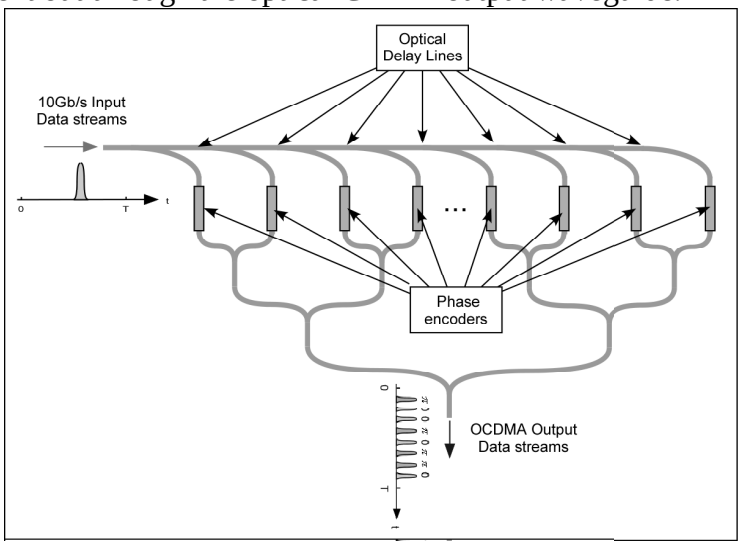

Figure 3.2, Schematic of the OSP circuit for a 10-chip OPTICAL CDMA encoder

The optical CDMA decoder module, shown in Figure 3.3, consists of optical-time lines, tunable phase-decoders, and a high-speed time-gate (~20ps). The high-speed time-gate only allows the optical auto-correlation main-lobe pass for individual data bits, thus effectively reduces the cross-correlation noises and thus increases the signal-to-noise ratio (SNR).

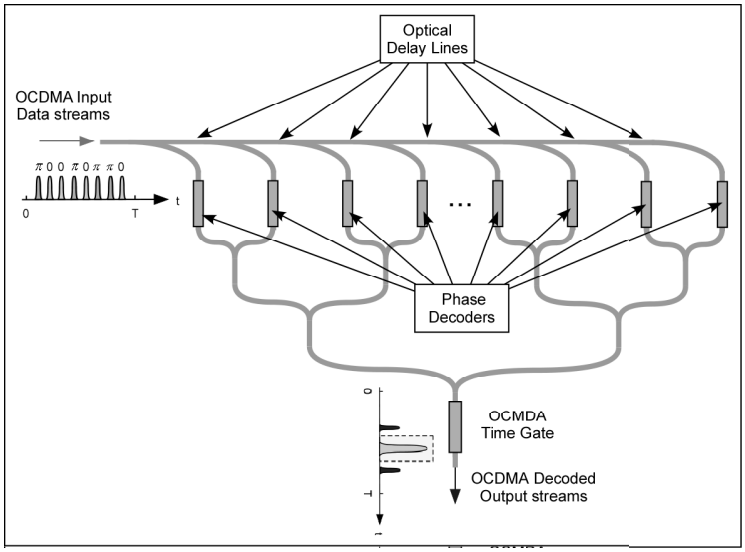

Figure 3.3, Schematic of the OSP circuit for a 10-chip OPTICAL CDMA decoder

The principle of the direct sequence encoding and decoding in time domain are shown in figure 3.2 and 3.3, respectively. In the encoder, each bit of the data signals is encoded by 10 time-resolved chip pulse code generates binary phase-shift keying (BPSK) signals called a code sequence. The code sequences can be written as:

$$X_k(t) = \sum_{m=0}^{N-1} b_m^k u(t - mT_c), \tag{1}$$

Where, b_m^k is the BPSK codes, T_c is the chip pulse width, and $u(t)$ is the pulse profile. The code sequences for individual channels are orthogonal, i.e.:

$$\begin{aligned} R(\tau) &= X_i(t) X_k(t - \tau) \\ &= \sum_{m=0}^{N-1} \sum_{n=0}^{N-1} b_n^i b_m^k u(t - mT_c) u(t - nT_c - \tau) = \delta_{i,k} \delta(\tau), \end{aligned} \tag{2}$$

Where, $R(\tau)$ is the channel correlation function. The encoded signal $f_i(t)$ for each channel is given by the convolution of the data signal $s(t)$ and the code $X(t)$:

$$\begin{aligned} f_i(t) &= s_i(t) \otimes X_i(t) \\ &= \sum_{m=0}^{N-1} \sum_{n=0}^{N-1} b_m^i u(t - mT_c) s_i(t - nT_s - mT_c), \end{aligned} \tag{3}$$

Where, T_s is the time duration for one signal bit. The total transmitted signal, $f(t)$, can be expressed as the summation of the encoded signal of each individual channel, i.e.:

$$f(t) = \sum_{i=1}^{M} f_i(t), \tag{4}$$

Where, M is the total number of channels in the OPTICAL CDMA system. The received signal, $r(t)$, contains both the transmitted signal, $f(t)$, and the noise, $n(t)$, accumulated during transmission, i.e.:

$$r(t) = f(t) + n(t), \tag{5}$$

In the receiver, the received signal, $r(t)$, is decoded by taking correlation with a specific code sequence as each individual channel. The decode sequences can be written as:

$$Y_k(t) = \sum_{m=0}^{N-1} d_m^k u(t - mT_c), \tag{6}$$

Where, d_m^k is also the BPSK codes. The code sequences for individual channels are also orthogonal. The decoded signal for each individual channel, $g_i(t)$, is given by the convolution of the received signal with the code sequence:

$$g_i(t) = r(t) \otimes Y_k(t) = f(t) \otimes C_{XY}(t), \tag{7}$$

Where, $C_{XY}(t)$ is the correction function between $X(t)$ and $Y(t)$.

Based on these equations, numerical simulation was performed for a 10gbit/s 10-chip OPTICAL CDMA system. The results were shown in figure 3.4 (a-g): (a) original channel 1 signal bits (NRZ format), (b) BPSK encoded channel 2 signal original channel 2 signal bits, (d) BPSK encoded channel 2 signal. The received signals are shown in (e), which contains the both BPSK encoded channel 1 and channel 2 signals plus the noise accumulated in the transmission. The noises are generated either from optical amplifiers or the inter-symbol-interference due to fiber dispersion. The decoded channel 1 and 2 signals are shown in (f) and (g) respectively. Note that, the original signals form channel 1 and 2 are separated and recovered.

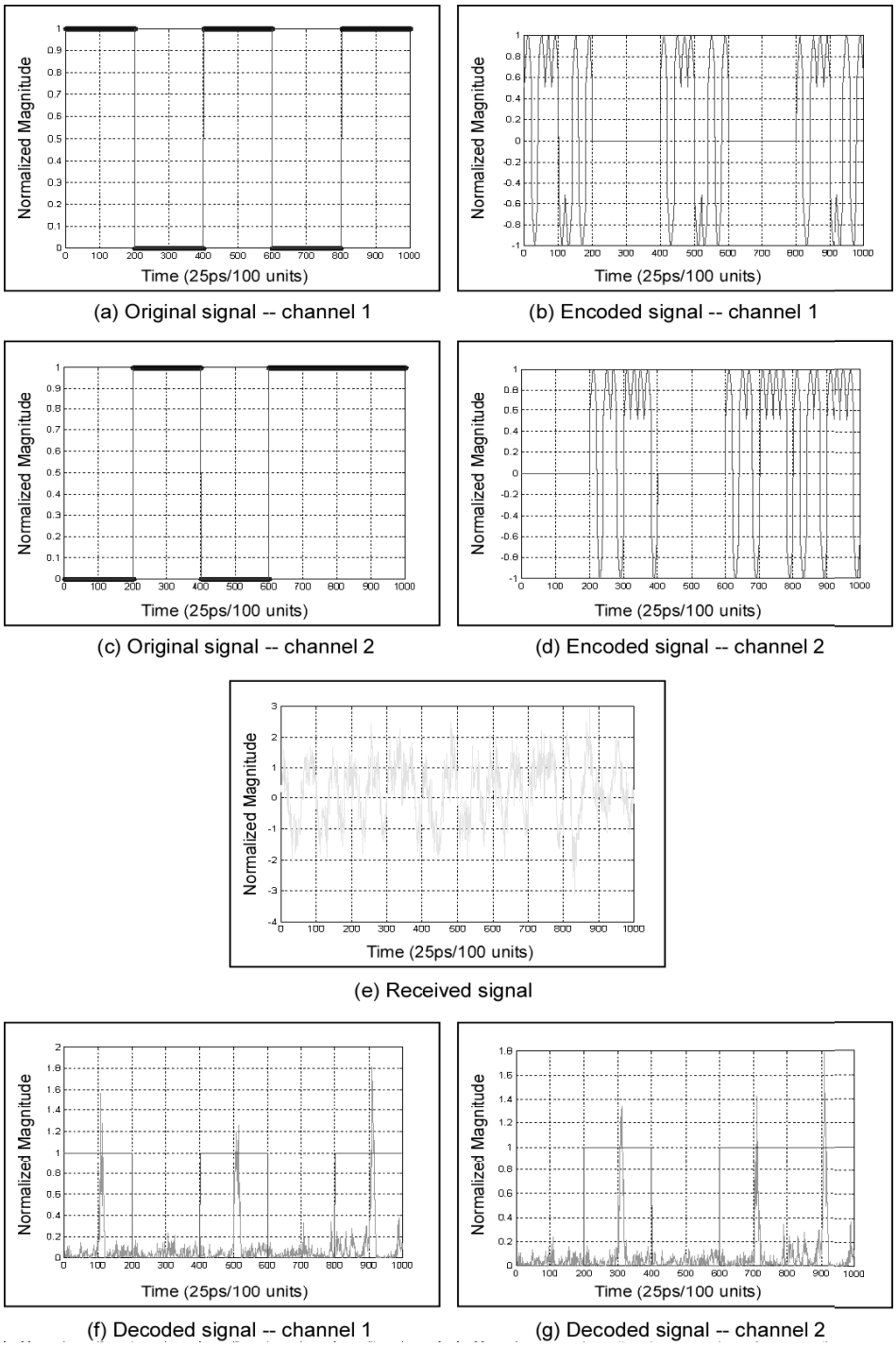

Figure 3.4 simulation of a 10Gbit/s OPTICAL CDMA system
(a) original channel 1 signal bits, (b) BPSK encoded channel 2 signal
(b) original channel 2 signal bits, (d) BPSK encoded channel 2 signal
(e) the received signal
(f) decoded channel 1 signal (g) decoded channel 2 signal

As shown in figure 3.4(f) and (g), the noise floor are due to the cross correlation of the code sequence. The signal-to-noise ratio (SNR) is given by [14]:

$$SNR = 4\left[\frac{N^3}{(K-1)(N^2+N-1)}\right], \qquad (8)$$

Where, N is the number of chips, and K is the number of simultaneous users. In order to increase the SNR, a time-gate, shown in figure 3.2, is incorporated in the decoder to only allow the optical auto-correlation main-lobe pass for individual data bits. The time-gate reduces the cross-correlation noises and thus effectively increases the signal-to-noise ratio (SNR), which therefore leads to an improved BER performance.

Polymer based high-speed unidirectional electro-optic (EO) modulator has the advantages of low insertion loss of < 1.0dB, monolithically integratable with other devices, including time-delay lines, combiner/splitters, and optical phase shifter arrays to form an polymer photonics integrated circuits. The EO modulator based time-gate, shown in figure 3.5, consists of a single waveguide for optical signal guiding, top and bottom modulating electrodes, and a planar dumping waveguide. The guiding multi-mode waveguide and the dumping planar waveguide, separated by a low-index polymer buffer layer, are designed to achieve phase-matches between the coupling mode of the guiding waveguide and the planar waveguide. The phase-mismatches ensure the optical beam in the guiding waveguide can be efficiently coupled to the dumping planar waveguide. The dumping planar waveguide was designed to be lossy (>-6.5 db/cm) such that optical energy coupled from the guiding multi-mode waveguide can be efficiently dumped out, thus a unidirectional coupling mechanism can be achieved. The eo induced index grating generates phase-mismatch and decreases the coupling from the guiding waveguide, and thus turns on the gate.

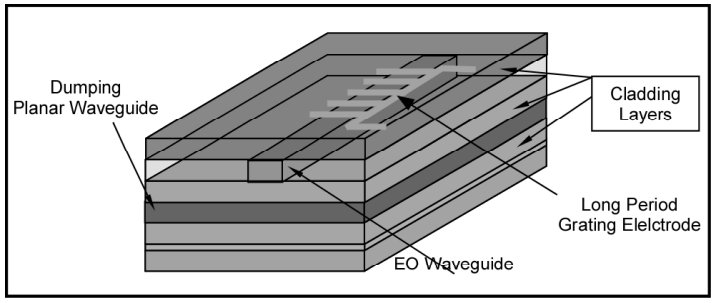

Figure 3.5, schematic structure of the high-speed time-gate based on the unidirectional EO modulator structure

The unidirectional coupling equations can be written as [15]:

$$2(i\beta_n - \alpha_n)\frac{dA_n}{dz} + \kappa_{mn}A_m(z)e^{(\alpha_m-\alpha_n)z}e^{i\Delta z} = 0, \qquad (9)$$

$$2(i\beta_m - \alpha_m)\frac{dA_m}{dz} + \kappa_{nm}A_n(z)e^{(\alpha_n-\alpha_m)z}e^{-i\Delta z} = 0, \qquad (10)$$

Where, κ_{mn} is the coupling constant between the guided modes of the guiding waveduide and the planar waveguide, $\Delta = \beta_m - \beta_n - \frac{2\pi}{\Lambda}$ is the phase-mismatch, Λ is the period of the grating, and β, α are the propagation constant and the loss coefficient, respectively. Ignoring the loss of the guiding waveguide, α_n, i.e. $\alpha_n \approx 0$, and solving the differential equations (9) and (10), one can get:

$$A_n(z) = e^{-\frac{i\Delta+\alpha}{2}z}\left[Ae^{(c+jd)z} + Be^{-(c+jd)z}\right], \tag{11}$$

$$c = \frac{1}{2}\mathrm{Re}\left[\sqrt{\alpha^2 - \Delta^2 - \frac{|\kappa|^2}{1+(\alpha_m/\beta_m)^2} + i\left[2\Delta\alpha_m + \frac{|\kappa|^2\alpha_m/\beta_m}{1+(\alpha_m/\beta_m)^2}\right]}\right], \tag{12}$$

$$d = \frac{1}{2}\mathrm{Im}\left[\sqrt{\alpha^2 - \Delta^2 - \frac{|\kappa|^2}{1+(\alpha_m/\beta_m)^2} + i\left[2\Delta\alpha_m + \frac{|\kappa|^2\alpha_m/\beta_m}{1+(\alpha_m/\beta_m)^2}\right]}\right], \tag{13}$$

Considering the boundary condition: $\frac{d}{dz}A_n(z)|_{z=0} = 0,$ one get:

$$B = A\frac{(-\alpha_m/2 + c) + j(d - \Delta/2)}{(\alpha_m/2 + c) + j(d + \Delta/2)}, \tag{14}$$

Substituting (4), (5) and (6) into (3), one get the intensity of the light:

$$I_n(z) = |A_n(z)|^2 = e^{-\alpha z}|A|^2\left|e^{(c+jd)z} + \frac{(-\alpha_m/2 + c) + j(d - \Delta/2)}{(\alpha_m/2 + c) + j(d + \Delta/2)}e^{-(c+jd)z}\right|^2, \tag{15}$$

The simulation results of the intensity of light in the guiding waveguies are shown in Figure 3.6. Notice that when phased-matched and the planar waveguide is lossy, high efficiency unidirectional coupling can be achieved. When the coupling is phase-mismatched, less than -1dB power coupling loss to the dumping waveguide can be obtained with the device length of 3.5cm.

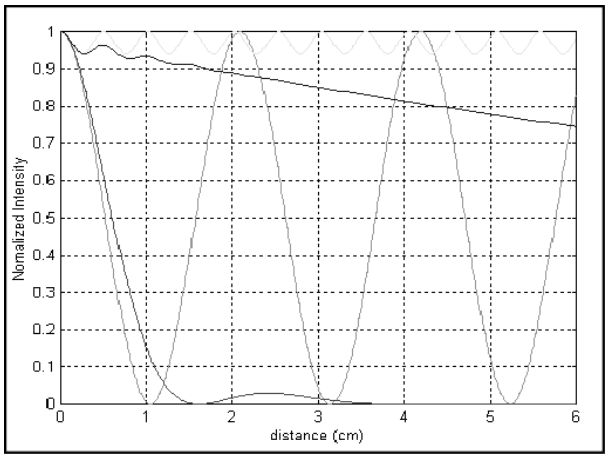

Figure 3.6, simulation results of the unidirectional coupling, green: phase-matched lossless; upper line: phase-mismatched lossless; lower line: phase-matched with loss of –

6.5dB/cm; middle line: phased-mismatched with loss of –6.5dB/cm, oscillating line: phase-matched, no loss.

By monolithically integrating accurate time-delay lines, tunable phase-encoders and high-speed time gate, the proposed optical CDMA encoder offers a unique solution for FTTH. It not only reduces costs associated with optical alignment and packaging, but also increases the optical SNR (OSNR) by reducing cross correlation noises through the integrated high-speed time-gate.

4. CONCLUSION

Polymer waveguide based photonics integrated circuits are promising in achieving high-performance all-optical signal processing circuits due to their large Electro-optic/thermo-optic coefficients and structure flexibility. The all-Optical signal processing circuits avoid the optical-to-electrical and electrical-to-optical conversions and thus eliminates the bandwidth constrains set by conventional electronics technologies. It will form key building blocks for the next generation ultra-high speed and dynamic multi-casting optical networks.

REFERENCE:

1. Lukasz Brzozowski and Edward H. (Ted) Sargent, *"All-Optical Analog-to-Digital Converters, Hardlimiters, and Logic Gates,"* J. Lightwave Technology, vol. 19, 114 (2001).
2. Behzad Razavi, *"Challenges in the Design of High-Speed Clock and Data Recovery Circuits,"* IEEE Communications Magazine, pp 94-101 (2002).
3. J. M. Senior, *Optical Fiber Communications, Principles and Practice*, 2nd ed. Cambridge, U.K.: Cambridge Univ. Press, 1992.
4. http://www.fcc.gov/realaudio/workshops.html
5. Scott A. Hamilton, Bryan S. Robinson, Thomas E. Murphy, Shelby Jay Savage, and Erich P. Ippen, *"100 Gb/s Optical Time-Division Multiplexed Networks,"* J. Lightwave Technol., vol. 22, pp. 2086–2100(2002).
6. Jen-Fa Huang, Chen-Mu Tsai, and Yu-Lung Lo, " Compensating Fiber Gratings for Source Flatness to Reduce Multiple-Access Interferences in Optical CDMA Network Coder/Decoders," *J. Lightwave Technol.*, vol. 22, pp. 739–745, March , 2004.
7. José Azaña, and Lawrence R. Chen, "Multiwavelength Optical Signal Processing Using Multistage Ring Resonators," IEEE Photonics Technology Lett., vol. 14, 654 (2002).
8. B. E. Little, J. S. Doresi, G. Steinmeyer, E. R. Thoen, S. T. Chu, H. A. Haus, E. P. Ippen, L. C. Kimerling, and W. Greene, *"Ultra-compact Si-SiO microring resonator optical channel dropping filters," IEEE Photon. Technol. Lett.*, vol. 10, 549 (1998).
9. H. J. S. Dorren, M. T. Hill, Y. Liu, N. Calabretta, A. Srivatsa, F. M. Huijskens, H. de Waardt, and G. D. Khoe, *"Optical Packet Switching and Buffering by Using All-Optical Signal Processing Methods,"* IEEE *J. Lightwave Technol.*, vol. 21, 2(2003).
10. Xuejun Lu**,** *"An Adaptive Optical Filter Based on Thermo-Optic (TO) Polymeric Waveguide Lattice Filters"*, Conference presentation, *PhotonicsWest* 2004, Jan. 24-29.

11. Spiekman, L.H.; Wiesenfeld, J.M.; Gnauck, A.H.; Garrett, L.D.; Van Den Hoven, G.N.; Van Dongen, T.; Sander-Jochem, M.J.H.; Binsma, J.J.M.; **"***Transmission of 8 DWDM channels at 20 Gb/s over 160 km of standard fiber using a cascade of semiconductor optical amplifiers***"** Photonics Technology Letters, IEEE, Volume: 12 Issue: 6 , June 2000. Page(s): 717 –719.

12. Monson H. Hayes, *"Statistical Digital Signal Processing and Modeling "*.
13. Takada, K.; Abe, M.; Shibata, T.; Okamoto, K.; *"10-GHz-spaced 1010-channel tandem AWG filter consisting of one primary and ten secondary AWGs";* IEEE Photonics Technology Letters, Vol. 6, 577 (2001).
14. M. E. Marhic, *"Coherent optical CDMA networks,"* J. Lightwave Technol., vol. 11, pp. 854–863, June 1993.
15. Xuejun Lu**,** Linghui Wu, Xuping Zhang, and Ray T. Chen, *"A Grating-assisted Electro-Optic Modulator Based on Polymeric Waveguide,"* submitted to Optical Engineering, 2004.